THE JOURNAL OF BIOLOGICAL CHEMISTRY VOL. 283, NO. 47, pp. 32968–32976, November 21, 2008

The Structure of YqeH

*AN AtNOS1/AtNOA1 ORTHOLOG THAT COUPLES GTP HYDROLYSIS TO MOLECULAR RECOGNITION**[S]

Received for publication, June 25, 2008, and in revised form, September 8, 2008 Published, JBC Papers in Press, September 18, 2008, DOI 10.1074/jbc.M804837200

Jawahar Sudhamsu[‡], **Gyu In Lee**[§], **Daniel F. Klessig**[§], **and Brian R. Crane**[‡1]

From the [‡]*Department of Chemistry and Chemical Biology, Cornell University, Ithaca, New York 14853 and* [§]*Boyce Thompson Institute for Plant Research, Ithaca, New York 14853*

AtNOS1/AtNOA1 was identified as a nitric oxide-generating enzyme in plants, but that function has recently been questioned. To resolve issues surrounding AtNOA1 activity, we report the biochemical properties and a 2.36 Å resolution crystal structure of a bacterial AtNOA1 ortholog (YqeH). *Geobacillus* YqeH fused to a putative AtNOA1 leader peptide complements growth and morphological defects of *Atnoa1* mutant plants. YqeH does not synthesize nitric oxide from L-arginine but rather hydrolyzes GTP. The YqeH structure reveals a circularly permuted GTPase domain and an unusual C-terminal β-domain. A small N-terminal domain, disordered in the structure, binds zinc. Structural homology among the C-terminal domain, the RNA-binding regulator TRAP, and the hypoxia factor pVHL define a recognition module for peptides and nucleic acids. TRAP residues important for RNA binding are conserved by the YqeH C-terminal domain, whose positioning is coupled to GTP hydrolysis. YqeH and AtNOA1 probably act as G-proteins that regulate nucleic acid recognition and not as nitric-oxide synthases.

AtNOS1 (*Arabidopsis thaliana* nitric-oxide synthase 1) was originally identified as a plant enzyme capable of producing nitric oxide (NO)[2] from the amino acid Arg (1). In plants, NO functions in many processes, including seed germination, hormone responses, respiration, root development, leaf expansion, fruit maturation, senescence, abiotic stress response, cell death, and disease resistance (2–5). In particular, the role of NO in plant-pathogen interactions has received considerable attention (6–8). Plant extracts generate NO and citrulline in an Arg-dependent manner, and this activity can be blocked by animal nitric-oxide synthase (NOS) inhibitors (9–14). Arg-dependent NO synthesis is important, because the well studied animal NOSs produce NO from this substrate in an active center that contains heme and tetrahydrobiopterin (15, 16). NOS inhibitors prevent some NO-mediated responses, such as ABA-induced stomatal closure (1), and also compromise the resistance to pathogens (17).

AtNOS1 was the second of two plant enzymes reported to catalyze the conversion of Arg to NO (1, 18), but in both cases, the results have not been reproduced (8, 19–21). AtNOS1 was identified from *A. thaliana* based on homology to a hypothetical snail NOS that appeared to synthesize NO (22). Despite virtually no sequence similarity with animal NOSs, mutation of the *AtNOS1* gene generates a growth phenotype that can be rescued by NO donor compounds. In addition, chemical probes sensitive to NO show reduced activation in the knock-out mutant (1). Genetic studies (23) further demonstrate that the *Atnos1* mutant is more susceptible to the pathogen *Pseudomonas syringae* than wild-type plants. However, consistent with our own results, several groups have stated that they cannot reproduce NO synthase activity with host-derived or recombinant AtNOS1, calling into question the true function of this protein and resulting in its redefinition as AtNOA1 (for nitric oxide-associated protein) (8, 21).

AtNOA1 is a 561-residue protein that contains four sequence motifs characteristic of GTP-binding proteins, such as p21-Ras, Rho, Rac, Cdc42, and Gα domains (24–26). However, the order of motifs in the protein sequence indicates an unusual circular permutation of the polypeptide found only in a small subclass of GTPases of poorly understood function (24). Proteins containing circularly permutated G motif (CPG) domains are prevalent in bacteria (YlqF, YqeH, YjeQ, YawG, and MJ1464) but can also be found in yeast, plants, and even humans (*e.g.* LSG1) (25). CPG domains also belong to the HAS GTPase subfamily, which have a hydrophobic amino acid substitution in the place of a key hydrophilic residue that participates directly in GTP hydrolysis (often a Gln or His residue). Whereas AtNOA1 conserves the central HAS GTPase region, the protein also contains additional N- and C-terminal domains, neither of which have any relationship to other members of this family, except the shorter YqeH (~360 amino acids). In fact, YqeH is likely to have a domain structure very similar to that of AtNOA1 (22.8% identity, 33.6% similarity, for the *Geobacillus stearothermophilus* YqeH-GsYqeH). Both proteins contain an N-terminal region that harbors four cysteines ($CX_2CX_{25-35}CX_2C$) and secondary structure motifs consistent with the treble clef family of zinc-binding proteins (24). The

* This work was supported, in whole or in part, by National Institutes of Health Grant 5R01GM067011 (to D. F. K.). This work was also supported by National Science Foundation Grant CHE-0749996 (to B. R. C.). The costs of publication of this article were defrayed in part by the payment of page charges. This article must therefore be hereby marked "*advertisement*" in accordance with 18 U.S.C. Section 1734 solely to indicate this fact.

[S] The on-line version of this article (available at http://www.jbc.org) contains supplemental Table 1 and Figs. 1 and 2.

The atomic coordinates and structure factors (code 3EC1) have been deposited in the Protein Data Bank, Research Collaboratory for Structural Bioinformatics, Rutgers University, New Brunswick, NJ (http://www.rcsb.org/).

[1] To whom correspondence should be addressed: G60 S.T.OLIN, Cornell University, Ithaca, NY 14853. Tel.: 607-254-8634; Fax: 607-255-1248; E-mail: bc69@cornell.edu.

[2] The abbreviations used are: NO, nitric oxide; NOS, nitric-oxide synthase; CPG domain, circularly permutated G motif domain.

conserved C-terminal regions of both AtNOA1 and YqeH have no detectable homology to any domain of known structure. All of these features are conserved in the rice (*Oryza sativa*) and tomato (*Solanum lycopersicum*) homologs of AtNOA1 (63.1 and 59.9% amino acid identity, respectively). The similarity between AtNOA1 and YqeH is even more striking if a putative N-terminal mitochondrial targeting motif (27) is excluded from the comparison (29% identity, 43% similarity). The unusual arrangement of GTPase signature motifs and the unusual pendant domains make AtNOA1/YqeH interesting not only in the context of NO signaling in plants but also for understanding G-protein structure and function.

The function of YqeH in bacteria is not well understood. Some members of the CPG family (*i.e.* YlqF) have been implicated in ribosome biogenesis (28–30), but they contain C-terminal RNA-binding domains not found in YqeH/AtNOA1. Both YlqF and YqeH are essential for cell growth in *Bacillus subtilis*. They have been shown to bind [α-^{32}P]GTP (31), and GTPase activity was demonstrated for YqeH (32). The *B. subtilis yqeH* mutant is lethal, whereas reduced YqeH expression increases chromosomal replication (31). YqeH participates in the biogenesis of the 30 S ribosome subunit (32) and assists in 50 S ribosome assembly (33). A high throughput screen in yeast found that a distant homolog of YqeH interacts with a ribosomal protein (31, 34, 35). There is currently little data available about AtNOA1/YqeH mammalian homologs, aside from some localization studies that place them in the mitochondria (27). Nevertheless, it is clear that these proteins form a unique family that is broadly represented in biology. Their role in NO metabolism may very well extend to additional organisms.

Factors involved in bacterial ribosome assembly are potential targets for new antibacterial drugs (36–39). The fact that YqeH is found in Gram-positive bacterial pathogens, coupled with the lethality caused by its deletion in *B. subtilis*, makes it attractive as a target for design of inhibitors. Molecular structures of YqeH with bound substrates and inhibitors could aid such efforts.

It has been previously indicated that AtNOA1 does not synthesize NO (8, 21), but no experimental data were published along with these reports. Furthermore, the putative GTPase activity of the enzyme has not been characterized, nor have its other biochemical properties. In an effort to address the issues surrounding the function of ANOA1, we report the 2.36 Å resolution crystal structure of the YqeH homolog from *G. stearothermophilus* and further investigate its biochemistry. We also show that these data are highly relevant to AtNOA1, because bacterial YqeH rescues growth and morphological defects of *Atnoa1* mutant plants. The combined results indicate that YqeH/AtNOA1 is very unlikely to have NO synthase activity and rather appears to be a unique regulator capable of coupling GTP hydrolysis to nucleic acid and/or protein recognition.

EXPERIMENTAL PROCEDURES

Materials—Sodium citrate and sodium chloride were obtained from Mallinckrodt, polyethylene glycol 5000 monomethyl ether was from Fluka, Tris was from Fisher, and all other chemicals were obtained from Sigma, unless otherwise noted.

Cloning and Expression of GsYqeH—The YqeH gene of *G. stearothermophilus* (ATCC strain number 12980) was amplified from genomic DNA by PCR (with Phusion polymerase from New England Biolabs) and cloned into the pET28 (Novagen) expression vector between NdeI and XhoI. GsYqeH was then expressed in *Escherichia coli* BL21(DE3) cells with an N-terminal His_6 tag. Proteins were purified using nickel-chelate chromatography and then size exclusion chromatography (Superdex 75) after removal of the His_6 tag with thrombin. GsYqeH was concentrated to ~12 mg/ml in 50 mM Tris, pH 7.5, 150 mM NaCl as estimated by the Bradford assay.

Selenomethionyl protein was overexpressed in *E. coli* B834(DE3) cells, which are auxotrophic for methionine (40). An overnight culture in LB was spun down, washed twice with autoclaved water, and then added to the L-selenomethionine growth medium (M9 minimal media supplemented with 19 standard amino acids and L-selenomethionine at 50 mg/liter), which was then incubated at 37 °C for 6 h after induction with isopropyl 1-thio-β-D-galactopyranoside before harvesting cells. The protein was purified as above. Dithiothreitol (10 mM) was present in all buffers. The Thr-Ala and Cys-Ser substitutions in *GsYqeH* were produced using the QuikChange mutagenesis kit from Stratagene.

GTPase Assays—The GTPase reactions were performed with 10 μM protein in a buffer that contained 50 mM Tris, pH 7.5, 150 mM NaCl, 1 mM $MgCl_2$, and 1 mM GTP at 37 °C. After 2 h of incubation, samples were boiled for 5 min and then centrifuged to separate precipitated protein. The supernatants were analyzed by reverse phase HPLC (absorbance at 260 nm) on a Waters Sunfire^{TM} C_{18} 5 μm, 4.5 × 250-mm column. The running buffer contained 100 mM NaH_2PO_4, pH 6.5, 10 mM tetrabutyl ammonium bromide, 0.2 mM NaN_3, 7.5% acetonitrile. Product elution times were compared with standards for GTP, GDP, and GMP.

Crystallization, Data Collection, and Model Building—Single crystals of diffraction quality were grown by vapor diffusion from 5–12 mg/ml protein in 50 mM Tris, pH 7.5, 150 mM NaCl. The reservoir was mixed 1:1 with protein solution and contained 100 mM sodium citrate pH 4.8–5.4 and 0–5% polyethylene glycol 5000 monomethyl ether. Native and L-selenomethionine GsYqeH crystals belonged to the $P2_1$ space group with cell dimensions 47.6 × 81.1 × 108.2 Å and β = 91.5°. Diffraction data for the native GsYqeH crystals (2.36 Å) were collected at CHESS beamlines F1 and F2 on a Q4 quantum CCD detector. Single wavelength anomalous diffraction data (2.5 Å) for L-selenomethionine crystals were collected at the APS beamline NE-CAT 24-BM on a Q315 Quantum CCD detector. The data sets were reduced and scaled using HKL2000 (41). The GsYqeH model (residues 97–369) was built manually using XFIT (42) and COOT (43) in a 2.5 Å map generated from the single wavelength anomalous diffraction data by SOLVE and RESOLVE (44). A more complete model (GsYqeH residues 57–369) was then placed in the unit cell, and refined against the native data set (2.36 Å resolution) with AMoRe (45) and CNS (46). The structure was adjusted with XFIT and COOT to $F_o - F_c$ and $2F_o - F_c$ maps. The addition of GDP and water molecules amid cycles of refinement produced the final model (R = 25.3%; R_{free} = 27.1%) (supplemental Table 1).

Structure Analysis Programs and Computer Graphics—Structural alignments of proteins/peptides were made with URMS (47). Structural homology searches were carried out with DALI (48). The Function Site Prediction Server was used to identify functionally important residues, which were considered significant if the generalized linear model score was >6.0 (49). Molscript (50) generated the molecular representations.

Complementation of Atnoa1 by yqeH—For constitutive expression of AtNOA1 in plants, the *AtNOA1* open reading frame was amplified by PCR from a cDNA template with primers that generated XbaI and SmaI sites at the 5′ and 3′ ends. The PCR product was cloned into plant transformation vector pF3PZPY122 (51). This resulted in pF3PZPY122:*AtNOA1*, which encodes recombinant AtNOA1 tagged with three tandem FLAG epitopes at the C terminus. A DNA fragment encoding the first 101 amino acids of AtNOA1 was amplified by PCR with primers conferring NheI and XbaI sites at the 5′ and 3′ ends and cloned into the XbaI site of pF3PZPY122 to make pF3PZPY122:*101AtNOA1*. Then the *yqeH* open reading frame was amplified by PCR, digested with XbaI, and ligated with pF3PZPY122:*101AtNOA1* linearized by XbaI and SmaI to generate the chimeric *yqeH* construct for the complementation experiment.

Agrobacterium strain LBA4404 was transformed with chimeric *yqeH* constructs and pF3PZPY122:*AtNOA1*, and the recombinants were screened in LB medium containing chloramphenicol (10 μg/ml). *Atnoa1* mutant plants were transformed by the floral dip method (52). The transgenic plants were selected for gentamicin resistance (50 μg/ml Murashige-Skoog media) and allowed to set seeds. The genotypes of T2 plants were confirmed by PCR analysis of genomic DNA for the knock-out of wild-type *AtNOA1* and chimeric *yqeH* and for constitutive expression of *AtNOA1* cDNA.

RESULTS AND DISCUSSION

GTP Hydrolysis by GsYqeH

Based on the sequence relationships to CPG domains and previous reports that *B. subtilis* YqeH could interact with and hydrolyze guanine nucleotides (31, 32), we tested the ability of GsYqeH to bind and hydrolyze GTP. Initially, GsYqeH showed little evidence of nucleotide hydrolysis by HPLC analysis of products, but upon the addition of a known facilitator of nucleotide exchange (200 mM ammonium sulfate) (53), GsYqeH converts GTP to GDP over a period of hours in a Mg^{2+}-dependent manner (supplemental Fig. 1). Similar findings were also made for AtNOA1 in a companion study that provides additional data for the GTP hydrolysis properties of this enzyme family (85).

A Zinc Binding Motif in GsYqeH

Sequence analysis and secondary structure prediction of YqeH homologs revealed an N-terminal motif found in the treble clef family of zinc finger domains (24). The treble clef motif is contained within diverse proteins whose functions range from the binding of nucleic acids, proteins, and small molecules to the catalysis of phosphodiester bond hydrolysis (54). Inductively coupled plasma analysis on GsYqeH, purified without the addition of zinc, identified zinc as the most prevalent metal ion in the sample (data not shown). Zinc was present at nearly stoichiometric levels compared with protein. Zinc also affects the hydrodynamic properties of GsYqeH. Gel filtration chromatography (Superdex G75) of a GsYqeH sample prepared separately from the one analyzed above produced an elution profile with two closely separated peaks at a volume consistent with the predicted molecular weight of the protein (supplemental Fig. 2). However, upon the addition of 300 μM zinc chloride (to 250 μM protein), the elution peak corresponding to the larger hydrodynamic radius disappeared, and all of the protein appeared with the smaller hydrodynamic radius (supplemental Fig. 2). Thus, a population of recombinant GsYqeH is deficient in zinc, and zinc binding converts the protein to a more compact form.

To identify the residues responsible for zinc binding, we sequentially mutated the conserved cysteine residues to serine in the treble clef domain. Single GsYqeH point mutants at C7S, C10S, or C39S, a double mutant C7S/C10S, and a triple mutant C7S/C10S/C39S were readily expressed and purified from *E. coli*. Proteins with the single and double substitutions eluted at the same position as zinc-bound native protein when expressed in rich media. However, the triple substitution C7S/C10S/C39S eluted as the zinc-free native protein and did not undergo any change in hydrodynamic radius when incubated with zinc (supplemental Fig. 2). Note that the single and double Ser substitutions may also disrupt zinc binding, but a compact structure could result from disulfide bonding. Thus, the small N-terminal domain of YqeH is indeed a zinc-binding domain and is very unlikely to also contain the cofactors necessary to catalyze the conversion of Arg to NO.

Absence of NO Synthesis Activity

Following previous reports on AtNOA1 (1), the Griess assay was employed in attempts to detect Arg conversion to NO and further oxidized species by YqeH. No NO production from GsYqeH was observed under any conditions (data not shown). These included the presence and absence of the animal NOS cofactors tetrahydrobiopterin and calmodulin and reductants supplied as peroxide or NADPH. Given that the structure of YqeH (see below) bears no resemblance to NOS and contains none of the NOS-essential cofactors or binding sites for them, it is consistent that the protein does not have NO synthase activity. Notably, in a companion study (85) extensive tests for NO synthesis activity and arginine binding by AtNOA1 were also all negative.

The Crystallographic Structure of GsYqeH (CPG and C-terminal Domains)

Overall Structure—Recombinant GsYqeH formed crystals that diffracted to 2.36 Å resolution. The structure (Fig. 1) was determined by a single wavelength anomalous diffraction experiment on L-selenomethionine-derivatized material (supplemental Table 1).

N-terminal Zinc-binding Domain—The N-terminal zinc-binding domain (residues 1–58) is absent in the electron density maps, despite the addition of excess $ZnCl_2$ during handling and no evidence for proteolysis in the crystals (as verified by SDS-PAGE). GDP that co-purified with the protein is found bound in the CPG domain.

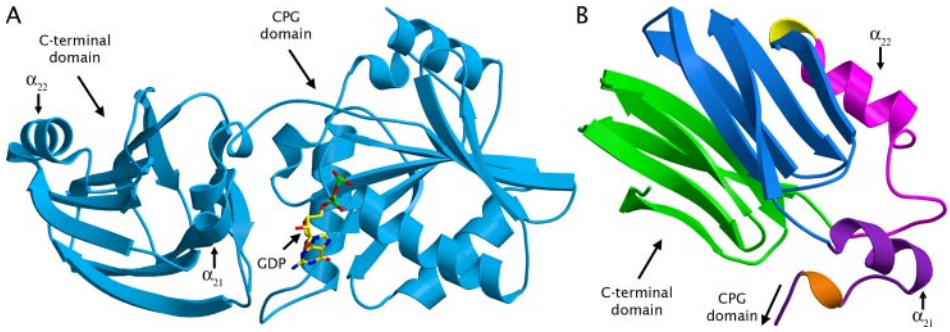

FIGURE 1. **Crystal structure of GsYqeH.** *A*, the CPG domain (*right*) has a central seven-stranded β-sheet surrounded by α-helices and binds GDP, which is exposed to the solvent on one side. The C-terminal domain (*left*) has a 2-fold pseudosymmetric β-fold. *B*, alternate view of the C-terminal domain. The domain starts (*bottom*) with a 3_{10}-helix (*dark orange*), followed by a coil (*purple*), α-helix (*purple*), five β-strands (*blue*), a 3_{10}-helix (*yellow*), an α-helix (*magenta*), coil (*magenta*), and five β-strands (*green*).

CPG Domain—The CPG domain has a typical G-protein fold with a central seven-stranded β-sheet (six parallel strands, one antiparallel strand) surrounded by six α-helices (Figs. 1 and 2*A*). In G-proteins, five sequence regions termed G1–G5 in the order they appear along the protein sequence, play important roles in nucleotide exchange, GTP hydrolysis, and conformational change (55, 56). G1–G5 are spatially close and are all associated with loop regions. G1–G4 are defined by conserved residues: G1 (G*XXXX*GK(S/T)), G2 (T), G3 (D*XX*G), G4 ((N/T)K*X*D) (24, 56). Interestingly, in YqeH, the G-regions of the CPG domain are rearranged as G4-G5-G1-G2-G3 in the linear sequence (Fig. 2*B*). However, this permutation allows for the same three-dimensional fold observed in canonical GTPases, such as the small G-protein Cdc42 (Protein Data Bank code 1ANO) (Fig. 2*A*), and the nucleotide-binding domains of larger G-proteins, such as Transducin (Protein Data Bank code 1GG2). This same permutation is also exhibited by the CPG domains of proteins such as YlqF from *B. subtilis* (Protein Data Bank code 1PUJ), YjeQ from *Thermotoga maritima* (Protein Data Bank code 1U0L), and YloQ from *B. subtilis* (Protein Data Bank code 1T9H). In GsYqeH, four of the five G-regions, except for G2 (Fig. 2*A*), overlap almost exactly with the same regions in GDP-bound Cdc42. The GsYqeH sequence permutation is produced by breaking the loop connecting β_3 and the 3_{10} helix in Cdc42 to generate the N and C termini of the domain and then connecting β_{14} to α_{15}, which correspond to the N termini (β_1) and C termini (α_6) of Cdc42, respectively (Fig. 2*B*).

Guanine Nucleotide Binding

The bound nucleotide (GDP) in GsYqeH is surprisingly exposed to solvent compared with that of other G-proteins. The α,β-phosphates of GDP interact with the so-called "P-loop," which is located between β_{14} and α_{16} (G1). Other regions in close contact with the GDP are the turns between α_{21} and β_{21}, β_{12} and α_{13} (G4), and β_{13} and α_{15} (G5) and the extended coil containing the G3 region, which is also known as Switch II (55). The protein provides multiple interactions to the bound nucleotide. Asp-109 hydrogen bonds to N2 and N3 of the guanine base, and the entire side chain of Lys-107 forms an aliphatic "bed" upon which the guanine ring lies. The hydroxyl group and backbone nitrogen of Ser-176 hydrogen bond to the β-phosphate, whereas the backbone nitrogen of Thr-177 hydrogen bonds to the α-phosphate. An ordered water molecule hydrogen bonds to both phosphates on the solvent-exposed side and to the carbonyl oxygen of Asn-172. GDP-bound YqeH does not provide any interactions for the hydroxyl groups of the ribose sugar ring.

GTP Binding and Hydrolysis Require Movement of Switch I

Regions of G-proteins called Switch I and II, which usually comprise G2 and G3, respectively, undergo conformational changes that trigger recognition of binding partners when G-proteins exchange GDP for GTP (55). In YqeH, the G2 region has atypical structure and is remote from the nucleotide. In contrast, G1 of Cdc42 is followed by α_1, which leads into a long coiled region that contains G2 and closely juxtaposes the bound GDP. In GsYqeH, the α_1-analog, α_{16}, does not connect to a G2-containing coil region but rather extends into a longer helix (Fig. 2*A*). The longer α_{16} continues into β_{15} before connecting to β_{16}, which corresponds to β_2 of Cdc42. Nevertheless, G2 of GsYqeH contains a conserved threonine residue (Thr-202) that participates in the hydrolysis mechanism of other GTPases. Involvement of YqeH Thr-202 in GTP hydrolysis would require a large rearrangement of G2 and regions surrounding Switch I. Interestingly, a similar movement of G2 has been observed in the Ran GTPases. Ran plays a vital role in the nuclear transport machinery (57, 58), where GTP hydrolysis regulates Ran-mediated interactions between importin-β-like transport receptors and diverse cargo, such as histones (59), small nuclear ribonucleoproteins (60, 61), heterogeneous nuclear ribonucleoproteins (62, 63), mRNA-binding proteins (64, 65), and tRNA (66, 67). In GDP-bound Ran, the G2 region that contains the catalytic Thr-42 (Thr-202 in GsYqeH) lies in a loop region, far from the nucleotide. (Fig. 3, *A* and *B*). GTP binding restructures G2 and allows Thr-42 to engage the β- and γ-nucleotide phosphates (Fig. 3*B*) (68, 69).

Mutational studies of two conserved Thr residues in YqeH G2 indicates that Switch I likely undergoes a conformational change similar to that observed for Ran. T201A has much less GTP hydrolysis activity compared with native GsYqeH, but T202A is completely inactive (Fig. 3*C*). In the Ran system, a family of Ran-binding domains (*e.g.* RanBP1) stabilizes the GTP-bound conformation of Switch I and assists in nucleotide hydrolysis (70, 71). Additional factors capable of playing a similar role could act as activators of YqeH GTPase activity.

GD(T)P Exchange May Position the C-terminal Domain via Switch II

Structural comparisons between YqeH and YlqF indicate that upon nucleotide exchange, Switch II (G3) of GsYqeH probably undergoes conformational changes that reposition the YqeH C-terminal domain. Both YlqF and YqeH belong to the CPG and HAS subfamilies of GTPases and have been

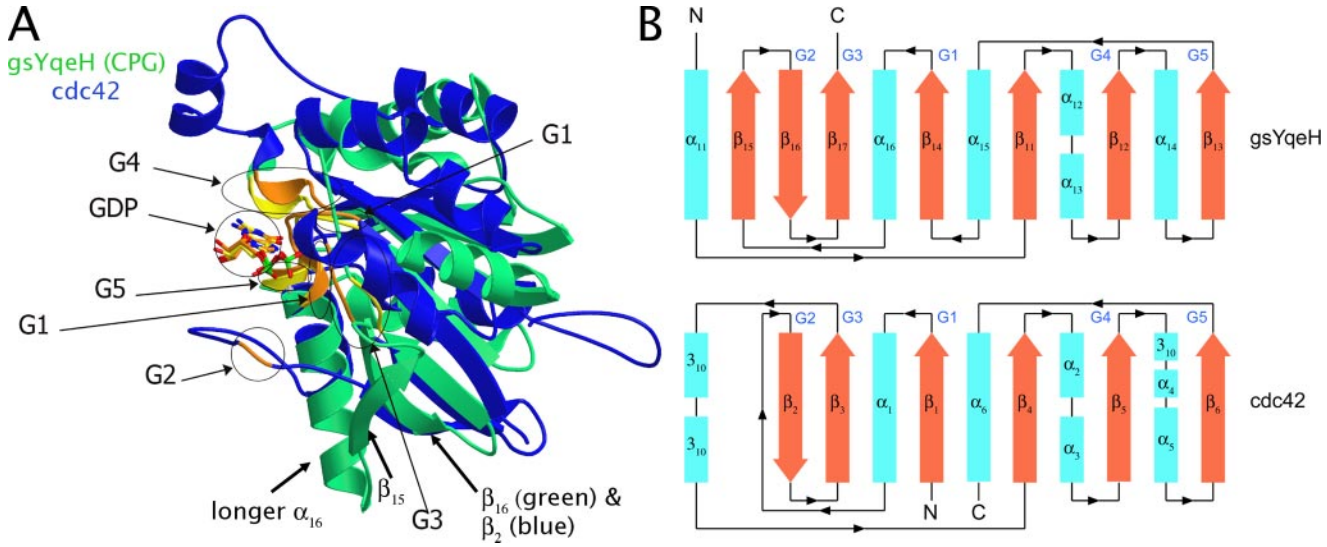

FIGURE 2. **Structure comparison of a canonical *versus* a circularly permuted GTPase.** *A*, structural superposition of GDP-bound forms of the GsYqeH CPG domain (*green*) and a canonical small G-protein Cdc42 (*blue*). Four of the five G-regions (except G2) overlap almost exactly, although their order in the linear sequence is permuted with respect to each other. There is a long coiled region between α_1 and β_2 in Cdc42, but in GsYqeH, the corresponding region continues as a helix, making α_{16} (GsYqeH) longer than α_1 (Cdc42). In GsYqeH, α_{16} continues as β_{15} before it joins to β_{16} in GsYqeH, which corresponds to β_2 in Cdc42. *B*, comparison of GsYqeH CPG domain and Cdc42 topologies. In the structural alignment, α_{11} in GsYqeH corresponds to the two 3_{10} helices in Cdc42 directly below it. β_{16} corresponds to β_2, β_{17} corresponds to β_3, etc. Cdc42 α_4 and the preceding 3_{10} helix are absent in GsYqeH.

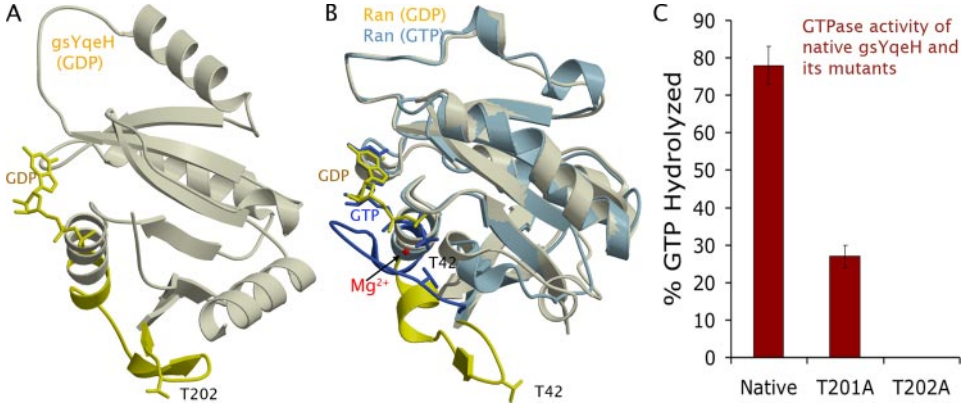

FIGURE 3. **Structure comparison of the GDP bound form of YqeH and the small GTPase Ran in GDP and GTP bound forms.** *A*, Switch I region (Thr-202) (*yellow*) in GsYqeH-GDP is located far from the active site. *B*, in Ran, conformational change in Switch I (Thr-42) brings the catalytically important residue close to the phosphates of GTP (*blue*), *versus* the GDP bound form (*yellow*). *C*, T202A substitution in YqeH completely abolishes GTPase activity, consistent with this residue moving into the active site on GTP binding. Assays were run in triplicate for 2 h.

implicated in *B. subtilis* ribosomal subunit assembly (28, 29, 33). In YqeH and YlqF, an Ile residue (222 in YqeH) of G3 substitutes for the catalytically important Gln/His found in many other GTPases. The crystal structure of *B. subtilis* YlqF bound to a nonhydrolyzable GTP analog (GMPPNP) (New York Structural GenomiX Research Consortium; Protein Data Bank code 1PUJ) reveals a C-terminal domain that is unlike that of YqeH (Fig. 4) but a CPG domain that is very similar. Furthermore, the G3 regions that connect the CPG to the C-terminal domains in both GsYqeH and BsYlqF are closely related in sequence (LYDTPGII in GsYqeH *versus* LLDTPGIL in BsYlqF), and both retain an Ile residue that resides next to the nucleotide phosphates. However, the conserved G3 regions have different conformations in the two proteins due to the presence of GDP in YqeH and a GTP analog in YlqF. In YlqF, the Ile side chain points away from the nucleotide, whereas in YqeH, the Ile-222 side chain flips into the pocket that would be occupied by γ-phosphate in YlqF (Fig. 4). It follows that GTP uptake by YqeH will displace Ile-222, and G3 will obtain a conformation similar to that found in GTP-YlqF. The resulting movement in the G3 linker would reposition the C-terminal domain (Fig. 4). This may be the signal conferred by GTP hydrolysis to switch the protein between different states of activity.

The YqeH C-terminal Domain

The C-terminal domain (residues 226–369) has a novel pseudo-2-fold symmetric β-sheet topology (Fig. 1*B*). The N- and C-terminal halves of the dyad are hereafter referred to as C_N and C_C. Both C_N and C_C contain a 3_{10}-helix, an α-helix, and five β-strands and are related by a 2-fold axis roughly parallel to the β-strands. C_N and C_C have low sequence identity (14%) but high structural similarity (C_α root mean square deviation: 2.1 Å for 55 of 70 residues) (Fig. 5, *B* and *D*).

Structural Homologs of Functional Relevance

A structural homolog search using DALI (48) returned no significant homologs when the C-terminal domain was queried against the entire Protein Data Bank (Z-score ≤ 2.0), indicating that, as a whole, this domain has a novel fold. However, the inherent 2-fold symmetry of the domain suggested that one-half of the dyad may represent a more fundamental folding unit (Fig. 5*B*). A search with this unit, C_C (residues 291–369) revealed a structural relationship to the protein TRAP (Trp

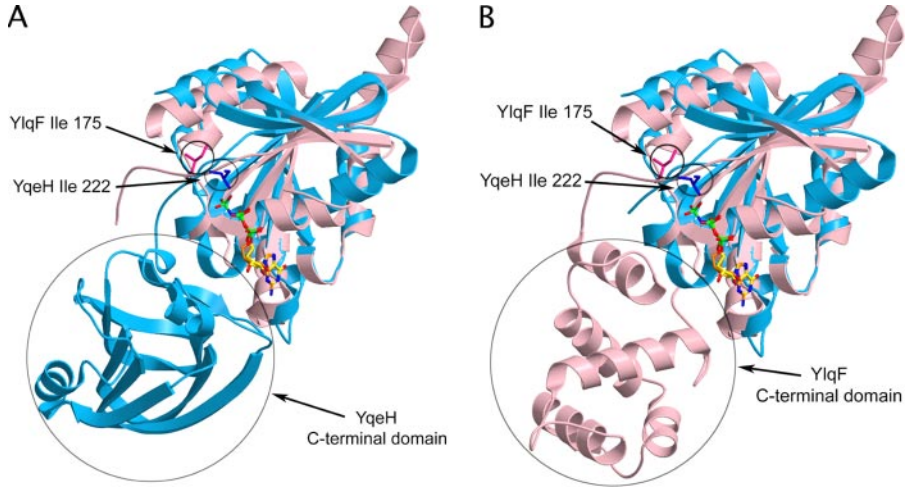

FIGURE 4. **GTP hydrolysis may change orientation of C-terminal domain.** Superpositions the CPG domains of GsYqeH (*blue*) and BsYlqF (*pink*) with the C-terminal domains of either BsYlqF (*A*) or GsYqeH (*B*) removed for clarity. Comparison of GTP-bound YlqF and GDP-bound YqeH indicates that GTP binding displaces the conserved Ile from the phosphate pocket and thereby reorients the C-terminal domain.

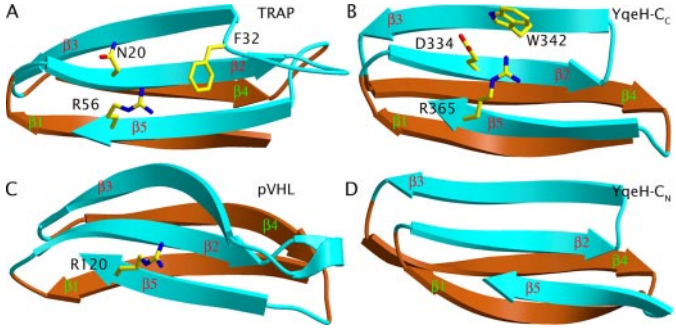

FIGURE 5. **The peptide/nucleotide recognition (*PNR*) fold.** The β-sandwich fold common to YqeH, TRAP, and pVHL contains five β-strands (β_1–β_5) and interacts with both peptides and nucleic acids. Shown are BsTRAP residues 8–58 (*A*), GsYqeH residues 318–365 (C_C) (*B*), human pVHL residues 73–121 (*C*), and GsYqeH residues 246–290 (C_N) (*D*). All of the above structures share structural similarity with the same topologies and C_α-root mean square deviations of 2.0–2.8 Å. In BsTRAP, residues Asn-20, Phe-32, and Arg-58 are involved in RNA binding. Analogous residues in GsYqeH are predicted to be of functional importance. pVHL also contains the Arg residue common to TRAP and YqeH. β_3 and β_4 in pVHL and in YqeH participate in peptide binding. β_4 and β_5 in TRAP participate in peptide binding. Analogous to TRAP, the solvent-exposed surface in YqeH formed by the strands β_2, β_3, and β_5 may bind RNA.

RNA-binding attenuating protein) from *B. subtilis* (*Z*-score = 4.0; length of match: 43 residues; C_α root mean square deviation: 2.0 Å; Fig. 5, *A* and *B*). When complexed with L-tryptophan, TRAP binds to the leader regions (11 (G/U)AG repeats) of the mRNA encoding the Trp biosynthetic enzymes, thereby inhibiting their translation (72, 73). RNA base triplets ((G/U)AG) wrap around the TRAP oligomer, which composes a ring of 11 subunits. The C-terminal domain of YqeH most likely does not bind Trp, since none of the TRAP Trp-binding residues are conserved in YqeH. Furthermore, due to the pseudosymmetry within the dyad, the C-terminal domain of YqeH cannot oligomerize like the TRAP molecules. Nonetheless, there are interesting correlations between the surface properties of the two proteins with respect to the function of TRAP. The YqeH C-terminal domain conserves some residues that have been shown to be important for RNA binding by TRAP (73). An invariant TRAP Arg-58 that binds (G/U)AG trinucleotide repeats aligns exactly with invariant Arg-365 in GsYqeH (Fig. 5, *A* and *B*). In both structures, these residues are completely exposed and appear to have no important function in stabilizing the structures of the respective domains. A highly conserved Asn residue (Asn-20) in TRAP that lies beside Arg-58 aligns well with a conserved aspartate (Asp-334) in GsYqeH (Fig. 5, *A* and *B*). A conserved Phe-32 in TRAP that π-stacks with the latter G in the (G/U)AG repeats mirrors conserved Trp-342 of GsYqeH (Fig. 5, *A* and *B*). The conserved Arg-365, Asn-334, Trp-342 triad of GsYqeH was also identified by a method independent of the TRAP relationship. Analysis of the YqeH structure with the "Function Site Prediction Server" (49), which filters sequence conservation due to functional relevance from conservation due only to structural constraints, also identified Arg-365, Asn-334, and Trp-342 as the highest scoring residues for functional relevance in C_C, along with a symmetry-related triad on C_N (Phe-260, Arg-266, Asp-268).

Structural Homology to pVHL

The DALI search with C_C also revealed homology to the Von Hippel-Lindau tumor repressor protein (pVHL) (*Z*-score: 3.9). pVHL is a regulator of HIF-α (hypoxia-inducible transcription factor), that activates genes involved in angiogenesis, apoptosis, and proliferation in response to hypoxia conditions (74, 75). pVHL binds to HIF-α when a critical HIF-α proline is hydroxylated by an oxygen-requiring prolyl-4-hydroxylase. pVHL then forms a ubiquitin-protein ligase complex along with elongin B, elongin C, Cul2, and Rbx1 that targets HIF-α for degradation (74, 75). Despite very low sequence similarity, C_N and C_C of YqeH have structural similarity to the β-domain of pVHL that recognizes the hydroxyprolyl-peptide (Fig. 5, *B–D*). Of the GsYqeH triads, only Arg-365 has an analog in Arg-120 of pVHL, (Fig. 5, *B* and *C*). Arg-120 is well conserved in the pVHL sequences but is not important for peptide recognition. In addition, none of the residues that are responsible for binding the hydroxylated peptide in pVHL are conserved by YqeH.

The Function Site Prediction Server identified three residue clusters on the surface of pVHL important for function. One cluster (Trp-88, Tyr-98, Leu-101, Pro-103, His-115, and Trp-117) includes those residues involved in binding hydroxylated HIF-1α. This region has been implicated in pVHL self-association (76) as well as the binding and inhibition of the transcriptional activator Sp1, which stimulates transcription of the hypoxia-related factors VEGF and GLUT-1 (76). Another conserved cluster (Leu-158, Leu-163, Ile-180, and Leu-184) comprises those residues important for elongin C binding. The third cluster (Arg-82, Phe-119, Asp-121, Val-130, and Ile-151) contains residues positioned on a face of the molecule similar to

where the clusters composing the TRAP/YqeH triad reside. Although the sequence positions of the Arg, Phe, and Asp residues are different from those in TRAP and YqeH, the similar composition of the triad in the three proteins may reflect a common RNA-binding function. There is some evidence that pVHL may destabilize certain mRNA, although the mechanism of action is not well understood (77–82).

The Peptide/Nucleotide Recognition Fold

The structural module common among YqeH, pVHL, TRAP, and AtNOA1 appears to be an adaptor capable of making interactions between proteins and nucleic acids. Within this β-sandwich topology, β_1 and β_4 form one sheet, and β_2, β_3, and β_5 form the other (Fig. 5). TRAP and pVHL interact with polypeptides through residues on β_4 and β_5 and on β_3 and β_4, respectively. In TRAP, the interaction is self-oligomerization (72); in pVHL, the interaction involves recognition of Sp1 (76) and hydroxylated HIF1-α (74, 75) and perhaps self-oligomerization (76). Analogous regions in the YqeH C-terminal domain also participate in polypeptide binding in the sense that they recognize each other, with β_3 of C_N binding β_4 of C_C and vice versa.

This module also binds RNA; hence, we refer to it as a peptide/nucleotide recognition (PNR) domain. In TRAP, the solvent-exposed surface of the β-sheet formed by β_2, β_3, and β_5 binds RNA and contains the triad Asn-20, Phe-32, and Arg-58. Similar residues on the analogous solvent-exposed surfaces of YqeH C_N and C_C may also bind RNA. In YqeH and AtNOA1, GT(D)P exchange may be functionally linked to RNA binding. In the GDP-bound GsYqeH, the predicted RNA-binding triad (Asp-334, Trp-342, and Arg-365) is shielded from solvent by the CPG domain. However, if exchange of GTP alters the connection between the CPG and peptide/nucleotide recognition (PNR) domains (Switch II) to a conformation similar to that observed in the GTP-bound form of YlqF (Fig. 4), these residues will become exposed; hence, their ability to bind targets (*e.g.* RNA) will be enhanced. The YqeH target may also activate YqeH by restructuring Switch I into a conformation appropriate for GTP hydrolysis. Given these analogies, it is interesting that the hydrolysis mechanism of the YqeH CPG domain is related to the mRNA/protein localization regulator Ran.

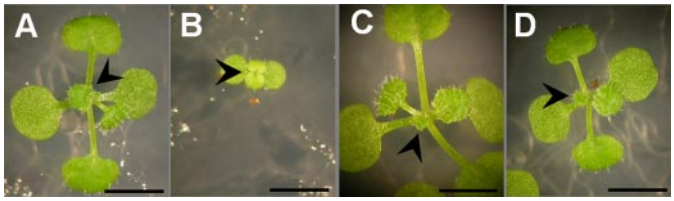

FIGURE 6. **Complementation of *Atnoa1* with chimeric *yqeH*.** *A*, wild type; *B*, *Atnoa1*; *C*, T2 generation of *Atnoa1* transformed with chimeric *yqeH*; *D*, T3 generation of *Atnoa1* transformed with wild type *AtNOA1*. The seed germination was synchronized by cold treatment. Photography was done 2 weeks after germination. The *size bars* correspond to 3 mm. The *arrowheads* point to emerging rosette leaves.

Complementation of Atnoa1 by Chimeric yqeH

Compared with wild type, *Atnoa1* mutant plants showed growth retardation and developed yellowish rosette leaves (1, 83, 84) (Fig. 6, *A* and *B*). The latter defect was rescued by application of NO donors (1, 84), which suggested a relationship between the morphological defect and NO deficiency in the mutant plants.

To test whether YqeH is an ortholog of AtNOA1, the bacterial protein was expressed in the *Arabidopsis Atnoa1* mutant plants. To facilitate proper targeting of YqeH in plants, a chimeric *yqeH* construct, which encodes GsYqeH with the first 101 amino acids of AtNOA1 fused to its N terminus, was used for the plant transformation. The chimeric *yqeH* complemented the morphological defects of *Atnoa1* as efficiently as wild-type AtNOA1 (Fig. 6, *C* and *D*). Both transgenic plants developed green rosette leaves, and their growth was comparable with that of wild-type plants. It has been recently reported that *B. subtilis yqeH* will also complement the growth and coloration phenotypes of *Atnoa1* mutant plants when it is fused to a peptide that targets it specifically to plastids/chloroplasts (84). This study further showed that native AtNOA1 is imported into chloroplasts both in leaves and *in vitro* (84). This provides an interesting contrast to the supposition that the leader peptide of AtNOA1 is for mitochondrial targeting (27) and supporting studies that found AtNOA1 in the mitochondria of roots (83). Thus, AtNOA1 may be important for the function of both prokaryotic derived organelles: plastids and mitochondria.

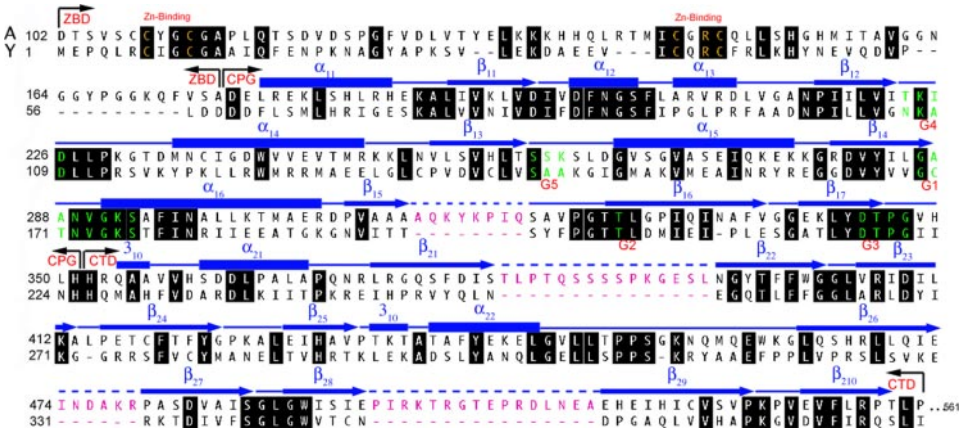

FIGURE 7. **Sequence alignment of AtNOA1 (*A*) and YqeH (*Y*).** 3_{10}-Helices and α-helices are denoted by *cylinders*, and β-strands are shown by *thick lines* with *arrows*. The protein is divided into three domains: the zinc-binding domain (*ZBD*), the circularly permuted G-domain (*CPG*), and the C-terminal domain (*CTD*). The residues that define the treble clef zinc site are shown in *yellow*, and the guanine nucleotide binding regions G1–G5 are shown in *green*. The insertions in the AtNOS1 protein sequence, as compared with the bacterial homolog (*magenta*), occur only in β-turn and loop regions.

Full Circle; Implications of GsYqeH for the Structure and Function of AtNOA1

The overall structure of AtNOA1 should be very similar to the structure of GsYqeH. Excluding the N-terminal leader peptide (27, 83, 84), the remaining ~100 extra residues in AtNOA1 as compared with the bacterial homologs occur as insertions in loop and β-turn

regions of the CPG and C-terminal domains (Fig. 7). Given the complementation data, we expect that AtNOA1 also acts as a switch protein that couples GTP hydrolysis to nucleic acid and/or protein binding. Recognition of ribosome components in plant mitochondria and/or plastids may be one of the functions of AtNOA1, given that depletion of YqeH leads to a defect in ribosome biogenesis in *B. subtilis*. How this would affect NO metabolism is not obvious (85), although it is worth noting that NO availability is closely linked to the concentration of oxygen radicals, of which the mitochondria and chloroplasts are major sources. Separate studies now show localization of AtNOA1 to both mitochondria (83) and chloroplasts/plastids (84). Further work aimed at linking AtNOA1 function to NO availability, as influenced by mitochondrial and chloroplast/plastid-associated processes, may prove fruitful.

Acknowledgments—We thank Dr. Nigel Crawford for providing Atnoa1 seeds and Dr. Magali Moreau for useful discussions.

REFERENCES

1. Guo, F.-Q., Okamoto, M., and Crawford, N. M. (2003) *Science* **302,** 100–103
2. Crawford, N. M., and Guo, F.-Q. (2005) *Trends Plant Sci.* **10,** 195
3. Crawford, N. M. (2006) *J Exp. Bot.* **57,** 471–478
4. Kaiser, W. M., Planchet, E., and Sonoda, M. (2004) *Nitric Oxide-Biol. Chem.* **11,** 37–37
5. Wendehenne, D., Durner, J., and Klessig, D. F. (2004) *Curr. Opin. Plant Biol.* **7,** 449–455
6. Delledonne, M. (2005) *Curr. Opin. Plant Biol.* **8,** 390
7. Mur, L. A. J., Carver, T. L. W., and Prats, E. (2006) *J. Exp. Bot.* **57,** 489–505
8. Crawford, N. M., Galli, M., Tischner, R., Heimer, Y. M., Okamoto, M., and Mack, A. (2006) *Trends Plant Sci.* **11,** 526–527
9. Cueto, M., HernandezPerera, O., Martin, R., Bentura, M. L., Rodrigo, J., Lamas, S., and Golvano, M. P. (1996) *FEBS Lett.* **398,** 159–164
10. Ninnemann, H., and Maier, J. (1996) *Photochem. Photobiol.* **64,** 393–398
11. Ribeiro, E. A., Cunha, F. Q., Tamashiro, W., and Martins, I. S. (1999) *FEBS Lett.* **445,** 283–286
12. Wendehenne, D., Pugin, A., Klessig, D. F., and Durner, J. (2001) *Trends Plant Sci.* **6,** 177–183
13. Durner, J., Wendehenne, D., and Klessig, D. F. (1998) *Proc. Natl. Acad. Sci. U. S. A.* **95,** 10328–10333
14. Lamotte, O., Gould, K., Lecourieux, D., Sequeira-Legrand, A., Lebrun-Garcia, A., Durner, J., Pugin, A., and Wendehenne, D. (2004) *Plant Physiol.* **135,** 516–529
15. Alderton, W. K., Cooper, C. E., and Knowles, R. G. (2001) *Biochem. J.* **357,** 593–615
16. Stuehr, D. J., Santolini, J., Wang, Z. Q., Wei, C. C., and Adak, S. (2004) *J. Biol. Chem.* **279,** 36167–36170
17. Delledonne, M., Xia, Y., Dixon, R. A., and Lamb, C. (1998) *Nature* **394,** 585
18. Chandok, M. R., Ytterberg, A. J., van Wijk, K. J., and Klessig, D. F. (2003) *Cell* **113,** 469–482
19. Klessig, D. F., Martin, G. B., and Ekengren, S. K. (2004) *Proc. Natl. Acad. Sci. U. S. A.* **101,** 16081
20. Klessig, D. F., Ytterberg, A. J., and van Wijk, K. J. (2004) *Cell* **119,** 445–445
21. Zemojtel, T., Frohlich, A., Palmieri, M. C., Kolanczyk, M., Mikula, I., Wyrwicz, L. S., Wanker, E. E., Mundlos, S., Vingron, M., Martasek, P., and Durner, J. (2006) *Trends Plant Sci.* **11,** 524–525
22. Huang, S., Kerschbaum, H. H., Engel, E., and Hermann, A. (1997) *J. Neurochem.* **69,** 2516–2528
23. Zeidler, D., Zahringer, U., Gerber, I., Dubery, I., Hartung, T., Bors, W., Hutzler, P., and Durner, J. (2004) *Proc. Natl. Acad. Sci. U. S. A.* **101,** 15811–15816
24. Anand, B., Verma, S. K., and Prakash, B. (2006) *Nucleic Acids Res.* **34,** 2196–2205
25. Reynaud, E. G., Andrade, M. A., Bonneau, F., Thi, B. N. L., Knop, M., Scheffzek, K., and Pepperkok, R. (2005) *BMC Biol.* **3,** 21
26. Zemojtel, T., Penzkofer, T., Dandekar, T., and Schultz, J. (2004) *Trend. Biochem. Sci.* **29,** 224–226
27. Zemojtel, T., Kolanczyk, M., Kossler, N., Stricker, S., Lurz, R., Mikula, I., Duchniewicz, M., Schuelke, M., Ghafourifar, P., Martasek, P., Vingron, M., and Mundlos, S. (2006) *FEBS Lett.* **580,** 455–462
28. Uicker, W. C., Schaefer, L., and Britton, R. A. (2006) *Mol. Microbiol.* **59,** 528–540
29. Matsuo, Y., Morimoto, T., Kuwano, M., Loh, P. C., Oshima, T., and Ogasawara, N. (2006) *J. Biol. Chem.* **281,** 8110–8117
30. Schaefer, L., Uicker, W. C., Wicker-Planquart, C., Foucher, A. E., Jault, J. M., and Britton, R. A. (2006) *J. Bacteriol.* **188,** 8252–8258
31. Morimoto, T., Loh, P. C., Hirai, T., Asai, K., Kobayashi, K., Moriya, S., and Ogasawara, N. (2002) *Microbiology (Read.)* **148,** 3539–3552
32. Loh, P. C., Morimoto, T., Matsuo, Y., Oshima, T., and Ogasawara, N. (2007) *Genes Genet. Syst.* **82,** 281–289
33. Uicker, W. C., Schaefer, L., Koenigsknecht, M., and Britton, R. A. (2007) *J. Bacteriol.* **189,** 2926–2929
34. Sickmann, A., Reinders, J., Wagner, Y., Joppich, C., Zahedi, R., Meyer, H. E., Schonfisch, B., Perschil, I., Chacinska, A., Guiard, B., Rehling, P., Pfanner, N., and Meisinger, C. (2003) *Proc. Natl. Acad. Sci. U. S. A.* **100,** 13207–13212
35. Huh, W. K., Falvo, J. V., Gerke, L. C., Carroll, A. S., Howson, R. W., Weissman, J. S., and O'Shea, E. K. (2003) *Nature* **425,** 686–691
36. Comartin, D. J., and Brown, E. D. (2006) *Curr. Opin. Pharmacol.* **6,** 453–458
37. Campbell, T. L., Daigle, D. M., and Brown, E. D. (2005) *Biochem. J.* **389,** 843–852
38. Wang, J., Galgoci, A., Kodali, S., Herath, K. B., Jayasuriya, H., Dorso, K., Vicente, F., Gonzalez, A., Cully, D., Bramhill, D., and Singh, S. (2003) *J. Biol. Chem.* **278,** 44424–44428
39. Margalit, D. N., Romberg, L., Mets, R. B., Hebert, A. M., Mitchison, T. J., Kirschner, M. W., and RayChaudhuri, D. (2004) *Proc. Natl. Acad. Sci. U. S. A.* **101,** 11821–11826
40. Doublie, S. (1997) *Macromol. Crystallogr. A* **276,** 523–530
41. Otwinowski, Z., and Minor, W. (1997) *Macromol. Crystallogr. A* **276,** 307–326
42. McRee, D. E. (1999) *J. Struct. Biol.* **125,** 156–165
43. Emsley, P., and Cowtan, K. (2004) *Acta Crystallogr. Sect. D Biol. Crystallogr.* **60,** 2126–2132
44. Terwilliger, T. (2004) *J. Synchrotron Radiat.* **11,** 49–52
45. Navaza, J., and Saludjian, P. (1997) *Macromol. Crystallogr. A* **276,** 581–594
46. Brunger, A. T., Adams, P. D., Clore, G. M., DeLano, W. L., Gros, P., Grosse-Kunstleve, R. W., Jiang, J. S., Kuszewski, J., Nilges, M., Pannu, N. S., Read, R. J., Rice, L. M., Simonson, T., and Warren, G. L. (1998) *Acta Crystallogr. Sect. D Biol. Crystallogr.* **54,** 905–921
47. Yona, G., and Kedem, K. (2005) *J. Comput. Biol.* **12,** 12–32
48. Holm, L., and Sander, C. (1996) *Science* **273,** 595–602
49. Cheng, G., Qian, B., Samudrala, R., and Baker, D. (2005) *Nucleic Acids Res.* **33,** 5861–5867
50. Kraulis, P. J. (1991) *J. Appl. Crystallogr.* **24,** 946–950
51. Feng, S. H., Ma, L. G., Wang, X. P., Xie, D. X., Dinesh-Kumar, S. P., Wei, N., and Deng, X. W. (2003) *Plant Cell* **15,** 1083–1094
52. Zhang, X. R., Henriques, R., Lin, S. S., Niu, Q. W., and Chua, N. H. (2006) *Nat. Prot.* **1,** 641–646
53. John, J., Sohmen, R., Feuerstein, J., Linke, R., Wittinghofer, A., and Goody, R. S. (1990) *Biochemistry* **29,** 6058–6065
54. Grishin, N. V. (2001) *Nucleic Acids Res.* **29,** 1703–1714
55. Milburn, M. V., Tong, L., deVos, A. M., Brunger, A., Yamaizumi, Z., Nishimura, S., and Kim, S. H. (1990) *Science* **247,** 939–945
56. Bourne, H. R., Sanders, D. A., and McCormick, F. (1991) *Nature* **349,** 117–127
57. Cook, A., Bono, F., Jinek, M., and Conti, E. (2007) *Annu. Rev. Biochem.* **76,** 647–671
58. Gorlich, D., and Kutay, U. (1999) *Annu. Rev. Cell Dev. Biol.* **15,** 607–660
59. Jakel, S., Albig, W., Kutay, U., Bischoff, F. R., Schwamborn, K., Doenecke, D., and Gorlich, D. (1999) *EMBO J.* **18,** 2411–2423

60. Fornerod, M., Ohno, M., Yoshida, M., and Mattaj, I. W. (1997) *Cell* **90,** 1051–1060
61. Gorlich, D., Dabrowski, M., Bischoff, F. R., Kutay, U., Bork, P., Hartmann, E., Prehn, S., and Izaurralde, E. (1997) *J. Cell Biol.* **138,** 65–80
62. Fridell, R. A., Truant, R., Thorne, L., Benson, R. E., and Cullen, B. R. (1997) *J. Cell Sci.* **110,** 1325–1331
63. Pollard, V. W., Michael, W. M., Nakielny, S., Siomi, M. C., Wang, F., and Dreyfuss, G. (1996) *Cell* **86,** 985–994
64. Aitchison, J. D., Blobel, G., and Rout, M. P. (1995) *J. Cell Biol.* **131,** 1659–1675
65. Aitchison, J. D., Blobel, G., and Rout, M. P. (1996) *Science* **274,** 624–627
66. Arts, G. J., Fornerod, M., and Mattaj, I. W. (1998) *Curr. Biol.* **8,** 305–314
67. Kutay, U., Lipowsky, G., Izaurralde, E., Bischoff, F. R., Schwarzmaier, P., Hartmann, E., and Gorlich, D. (1998) *Mol. Cell* **1,** 359–369
68. Kent, H. M., Moore, M. S., Quimby, B. B., Baker, A. M., McCoy, A. J., Murphy, G. A., Corbett, A. H., and Stewart, M. (1999) *J. Mol. Biol.* **289,** 565–577
69. Vetter, I. R., Nowak, C., Nishimoto, T., Kuhlmann, J., and Wittinghofer, A. (1999) *Nature* **398,** 39–46
70. Petersen, C., Orem, N., Trueheart, J., Thorner, J. W., and Macara, I. G. (2000) *J. Biol. Chem.* **275,** 4081–4091
71. Seewald, M. J., Korner, C., Wittinghofer, A., and Vetter, I. R. (2002) *Nature* **415,** 662–666
72. Antson, A. A., Dodson, E. J., Dodson, G., Greaves, R. B., Chen, X. P., and Gollnick, P. (1999) *Nature* **401,** 235–242
73. Yang, M., Chen, X. P., Militello, K., Hoffman, R., Fernandez, B., Baumann, C., and Gollnick, P. (1997) *J. Mol. Biol.* **270,** 696–710
74. Min, J. H., Yang, H. F., Ivan, M., Gertler, F., Kaelin, W. G., and Pavletich, N. P. (2002) *Science* **296,** 1886–1889
75. Hon, W. C., Wilson, M. I., Harlos, K., Claridge, T. D. W., Schofield, C. J., Pugh, C. W., Maxwell, P. H., Ratcliffe, P. J., Stuart, D. I., and Jones, E. Y. (2002) *Nature* **417,** 975–978
76. Cohen, H. T., Zhou, M., Welsh, A. M., Zarghamee, S., Scholz, H., Mukhopadhyay, D., Kishida, T., Zbar, B., Knebelmann, B., and Sukhatme, V. P. (1999) *Biochem. Biophys. Res. Commun.* **266,** 43–50
77. Iliopoulos, O., Levy, A. P., Jiang, C., Kaelin, W. G., and Goldberg, M. A. (1996) *Proc. Natl. Acad. Sci. U. S. A.* **93,** 10595–10599
78. Levy, A. P., Levy, N. S., and Goldberg, M. A. (1996) *J. Biol. Chem.* **271,** 25492–25497
79. Pioli, P. A., and Rigby, W. F. C. (2001) *J. Biol. Chem.* **276,** 40346–40352
80. Ross, J. (1995) *Microbiol. Rev.* **59,** 423–450
81. Shaw, G., and Kamen, R. (1986) *Cell* **46,** 659–667
82. Datta, K., Mondal, S., Sinha, S., Li, J. P., Wang, E. F., Knebelmann, B., Karumanchi, S. A., and Mukhopadhyay, D. (2005) *Oncogene* **24,** 7850–7858
83. Guo, F. Q., and Crawford, N. M. (2005) *Plant Cell* **17,** 3436–3450
84. Flores-Perez, U., Sauret-Gueto, S., Gas, E., Jarvis, P., and Rodriguez-Concepcion, M. (2008) *Plant Cell*, in press
85. Moreau, M., Lee, G. I., Wang, Y., Crane, B. R., and Klessig, D. F. (2008) *J. Biol. Chem.* **283,** 32957–32967